Al-Nahrain Journal for Engineering Sciences

Al-Nahrain J. Eng. Sci. 29(2) 319-326, 2026
Original Article

Synergistic Effects of Hybrid Nano-Calcium Carbonate and Nano-Talc Fillers on the Electrical, Thermal, and Morphological Properties of Epoxy-Glass Fiber Composites

Nishant Yadaorao Bhore[1], Prashant Vishwasrao Thorat [2] and Mangesh Shamrao Deshmukh[3]●.

1,2,3Department of Chemical & Polymer Engineering, College of Engineering and Technology, Akola, MH, India 444104

●*These authors contributed equally to this work*

DOI: https://www.doi.org/10.29194/NJES.29020319

Received: Aug. 25, 2025 **Revised:** Oct. 2, 2025 **Accepted:** Feb. 10, 2026 **Published:** June 20, 2026

Abstract

This research investigates the influence of single and hybrid mineral nanofillers on the morphological, thermal, and electrical properties of epoxy-based glass fiber composites. Nanocomposites were fabricated using hand lay-up technique, incorporating nano-calcium carbonate ($CaCO_3$) and nano-talc with particle size of 50 to 100 nm into an epoxy matrix with 5-ply E-glass/S-glass fiber. The study evaluates composites with 2-8 wt% of nano-$CaCO_3$, and hybrid systems containing nano-$CaCO_3$ (2-8 wt%) and nano-talc (1-4 wt%). Morphological analysis via Scanning Electron Microscopy (SEM) assessed nanofiller dispersion, while thermal properties were analyzed using Differential Scanning Calorimetry (DSC) for glass transition temperature (Tg). Electrical performance was evaluated through dielectric breakdown voltage (ASTM D149) and surface resistivity (ASTM D257). SEM analysis showed filler dispersion depended on concentration, with optimal distribution at 4-6 wt% before significant agglomeration at higher concentrations. DSC results revealed increased Tg with nanofillers, peaking for the composite with 6 wt% $CaCO_3$ and 3 wt% talc, indicating enhanced thermal stability. The dielectric breakdown voltage peaked at 17.6 kV for 2 wt% $CaCO_3$ and 1 wt% talc composite, while surface resistivity was highest for 4 wt% $CaCO_3$ and 2 wt% talc ($73.74\times1012\Omega$). All formulations maintained UL 94 V-1 flammability rating. The study concludes that the synergistic interaction between nano-$CaCO_3$ and nano-talc enables significant tailoring of thermal and electrical properties for advanced applications.

Keywords: *Epoxy Nanocomposites, Hybrid Fillers, Calcium Carbonate, Talc, Electrical Properties, Thermal Analysis, Morphology*

Corresponding author: Provide the corresponding author information and publisher here. E-mail address: nishantbhore@gmail.com

1. Introduction

Polymer composites, which are composed of multiple distinct components, have become essential in contemporary engineering owing to their lightweight nature, enhanced strength, and durability. Their applications extend across numerous high-performance sectors, including automotive, aerospace, defense, and marine industries [1-3]. The fundamental structure of a composite consists of a continuous matrix phase that binds to the reinforcing phase. Although the matrix and reinforcement provide inherent properties, the strategic incorporation of fillers has been recognized as a valuable approach to enhance specific characteristics and introduce new functionalities [4]. The geometric attributes, surface area, and chemical composition of these fillers can significantly modify the final properties of polymeric composites, often while simultaneously reducing material costs [5,6].

A prominent and emerging trend in this field is the development of nanocomposites that incorporate fillers with at least one dimension on the nanoscale (1-100 nm) [7]. The primary objective of using these nanofillers is to leverage their exceptionally high surface-area-to-volume ratio to maximize their interaction with the polymer matrix, thereby improving properties such as mechanical strength and thermal stability at very low loading levels. Among the various nanofillers, mineral-based nanoparticles such as nano-clays, silica, calcium carbonate ($CaCO_3$), and talc have garnered significant interest [8-11]. They offer a compelling combination of performance enhancement, cost-effectiveness, and processability compared to alternatives, such as carbon nanotubes (CNTs) or graphene, which can be limited by high costs, dispersion challenges, and inherent conductivity, making them unsuitable for dielectric applications [12,13].

Epoxy resins belong to a category of high-performance thermosetting polymers extensively utilized as matrix materials in advanced composites. They are well known for their exceptional adhesive properties, outstanding mechanical strength, excellent resistance to chemicals, and thermal stability [14,15]. These attributes make the epoxy an ideal choice for high-performance applications. Incorporating mineral nanofillers into epoxy matrices has been demonstrated to significantly enhance the material properties [16]. For example, the size and shape of nanoparticles play a crucial role; particles with high aspect ratios and smaller sizes typically result in better reinforcement owing to their increased interfacial area [17]. However, realizing these advantages relies heavily on overcoming the natural tendency of nanoparticles to clump together owing to strong van der Waals forces. Therefore,

modifying the surfaces of these nanofillers is essential to ensure compatibility with the organic polymer matrix and achieve even dispersion [18]. Methods such as treatment with silane coupling agents or fatty acids (e.g., stearic acid) are used to convert hydrophilic filler surfaces to become more organophilic, thereby enhancing interfacial adhesion and stress transfer [19-21].

Among the diverse ranges of mineral fillers, nano-calcium carbonate ($CaCO_3$) and nano-talc offer distinct advantages. Spherical or equiaxed Nano-$CaCO_3$ is favored due to its cost-effectiveness, low toxicity, and capacity to enhance the stiffness and impact strength [22,23]. Nano-talc, a hydrated magnesium silicate characterized by a lamellar (plate-like) structure, serves as an excellent reinforcing agent, known to augment stiffness, thermal stability, and barrier properties [24]. Although numerous studies have examined these nanofillers individually in epoxy, a notable research gap persists in the literature concerning the synergistic effects of combining $CaCO_3$ and Talc as a hybrid nanofiller system within an epoxy-glass fiber matrix [25]. Such a hybrid system could theoretically achieve a unique balance of properties, wherein the stiffness enhancement from nano-talc complements the toughness improvements from nano-CaCO3 [26].

This study seeks to address the existing gap by fabricating and thoroughly characterizing a series of epoxy-based glass fiber nanocomposites. This study primarily investigated the impact of incorporating single-filler (nano-CaCO3) and hybrid-filler (nano-$CaCO_3$ and nano-talc) systems on the resultant properties of the composite. The main objective is to establish definitive structure-property relationships by correlating the observed morphology with the thermal and electrical performance. This study provides an in-depth analysis of the fabricated single-filler nanocomposites and hybrid composites and discusses their thermal stability (via DSC), flammability, and electrical insulation capabilities (dielectric strength and surface resistivity), which are critical for applications in electronics, power systems, and automotive components.

2. Experimental Procedure

2.1. Materials

Materials required for the experimental work with their key specifications are listed in Table 1.

Table 1. List of Materials with Their Key Specification.

Material Category	Trade Name / Type	Supplier	Key Specifications
Matrix Resin	Lapox L-12 (DGEBA)	M/s Atul Ltd., Mumbai, India	Viscosity: 11,410 mPa·s @ 25°C Epoxy Value: 5.30 Eq/kg
Hardener	Lapox K-6 (Aliphatic Polyamine)	M/s Atul Ltd., Mumbai, India	Low viscosity Room temperature curing Mixing Ratio: 100:10 (Resin:Hardener)
Reinforcement 1	E-Glass Fiber (Chopped Strand Mat)	M/s 3B Goa Glass Fiber, India	Areal Density: 100g/m²
Reinforcement 2	S-Glass Fiber (Woven Mat)	M/s Go Green Products, Chennai, India	Areal Density: 100g/m² High tensile strength
Nanofiller 1	Nano-Calcium Carbonate ($CaCO_3$)	M/s Nano Research Lab, Jamshedpur, India	Particle Size: 50–100 nm Purity: 99.5% Surface Treatment: Stearic Acid
Nanofiller 2	Nano-Talc (Hydrous Magnesium Silicate)	M/s Nano Research Lab, Jamshedpur, India	Particle Size: 50–100 nm Purity: 99.5% Surface Treatment: Stearic Acid

2.2. Fabrication of Nanocomposites

A multistep fabrication process was employed, as illustrated in Fig.1. This is discussed below.

Step 1: Nanofiller Dispersion. Prior to use, the nano-$CaCO_3$ and nano-talc powders were dried in a hot air oven at 70°C for 2 h to remove any adsorbed moisture that could interfere with the epoxy curing reaction. The required weight percentage of dried nanoparticles was then added to the Lapox L-12 epoxy resin. A two-stage dispersion protocol was implemented to de-agglomerate the fillers. First, the mixture was subjected to ultrasonication in a bath for 2 h at 28°C to break down the large agglomerates via high-frequency pressure waves. This was immediately followed by high-shear mechanical stirring at 2000 RPM for 1 h to ensure macroscopic homogeneity of the suspension.

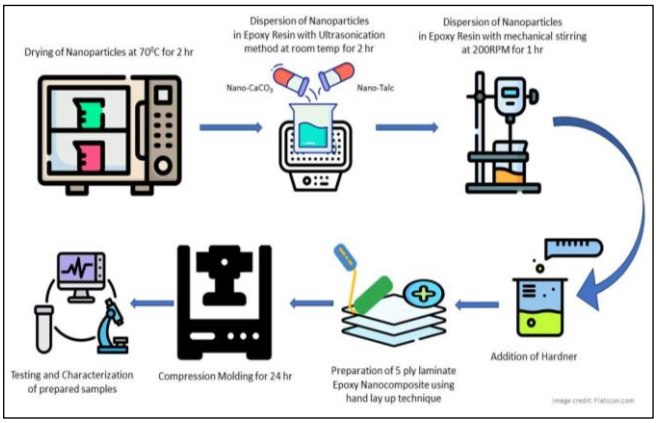

Figure 1. Schematic Diagram Illustrating the Preparation Steps for the Epoxy-Based Hybrid Nanocomposites.

Step 2: Laminate Fabrication and Curing. After achieving a stable dispersion, a stoichiometric amount of Lapox K-6 hardener was added and mixed gently to initiate the curing process. The composite laminates were fabricated in a 20 × 20 cm mold using a manual hand lay-up technique. A specific 5-ply hybrid stacking sequence of E-glass/S-glass/E-glass/S-glass/E-glass was used for all formulations. Each fiber mat was systematically and thoroughly impregnated with the prepared epoxy-nanofiller mixture.

Step 3: Curing. The completed wet laminate was placed under a 5-ton capacity compression screw jack for 24 h at ambient temperature. This final step served to consolidate the plies, expel trapped air, and allow the epoxy resin to fully cure into a rigid thermoset solid.

2.3. Experimental Formulations

To systematically study the effects of single and hybrid fillers, nine distinct formulations were prepared (Table 2). The control sample, EP, contained no nanofiller. The EPC series (EPC1-EPC4) contained only nano-$CaCO_3$ at increasing concentrations. The

EPCT series (EPCT1-EPCT4) contained a hybrid system of nano-$CaCO_3$ and nano-talc.

Table 2. Composition of the Fabricated Hybrid Nanocomposite Formulations.

Formulation Code	Nano $CaCO_3$ Concentration (wt% relative to epoxy)	Nano Talc Concentration (wt% relative to epoxy)
EP	0	0
EPC1	2	0
EPC2	4	0
EPC3	6	0
EPC4	8	0
EPCT1	2	1
EPCT2	4	2
EPCT3	6	3
EPCT4	8	4

2.4. Characterization Methods

The cured composite laminates were machined into standard specimens for characterization tests.

2.4.1 Morphological Analysis: The fracture surface morphology was examined using a JEOL 6390LA Scanning Electron Microscope (SEM). The samples were cryo-fractured after being submerged in liquid nitrogen to create a brittle fracture surface that was representative of the internal structure. The fractured samples were mounted on aluminium stubs and sputter-coated with a thin layer of gold to make them conductive and to prevent electrostatic charging. Images were captured at various magnifications to assess filler dispersion, agglomeration, and interfacial adhesion.

2.4.2 Thermal Characterization:

Differential Scanning Calorimetry (DSC): The glass transition temperature (Tg) was determined using a Shimadzu DSC-60 Plus calorimeter. Samples (~5 mg) were heated from room temperature to 300°C at a rate of 20°C/min under a nitrogen purge (50 ml/min). Tg was identified as the midpoint of the step change in the heat flow-versus-temperature curve.

Flammability: Flammability characteristics were assessed using a PLC-23A Flammability Tester, according to the UL 94 standard. This test involves subjecting a standard specimen to a controlled flame and observing its burning behavior, including the self-extinguishing time and dripping of the flaming particles, to assign a classification (e.g., V-0, V-1, and V-2).

2.4.3 Electrical Characterization:

Dielectric Breakdown Voltage (BDV): Measurements were performed according to ASTM D149, using an ARCON DBT-100 tester. Square samples (10 × 10 cm) were placed between the two electrodes in an insulating oil bath. The voltage was increased at a uniform rate until electrical breakdown occurred. The dielectric strength (kV/mm) was calculated by dividing the breakdown voltage by sample thickness.

Surface Resistivity: Measurements were conducted according to ASTM D257 on disc-shaped samples (10 cm diameter) using a Million Megohmmeter (Model LS-3BM). A direct voltage was applied for 60 s across the concentric ring electrodes, and the resistance to the current flow along the surface was measured. The results are expressed in ohms per square (Ω/sq).

3. Results and Discussion

3.1. Morphological Analysis (SEM)

The dispersion of nanofillers within the polymer matrix and the quality of the filler-matrix interface are paramount, as they directly dictate the macroscopic properties of the composite. Scanning Electron Microscopy of cryo-fractured surfaces provides crucial qualitative insights into these microstructural features.

3.1.1. Neat Epoxy Composite (EP) SEM micrographs of the control sample (EP), shown in Figure 2, reveal the baseline morphology. The glass fibers were visible as smooth cylindrical rods. In some areas, clean fiber pull-out was observed, indicating regions of relatively weak adhesion between the fiber and unmodified epoxy matrix. The matrix itself appears smooth and homogeneous, which is characteristic of a neat polymer fracture surface. As expected, no particulate features were observed. This morphology serves as a reference for evaluating the changes induced by the nanofillers.

3.1.2. Single-Filler Nanocomposites (EPC Series)

The introduction of nano-$CaCO_3$ significantly altered the fracture surface morphology, as seen in the EPC series (Fig. 3).

EPC1 (2 wt% $CaCO_3$): At a low loading of 2 wt%, the $CaCO_3$ nanoparticles appeared as small, discrete white dots dispersed on the fiber surfaces and within the matrix. The dispersion was relatively uniform, with minimal signs of large-scale agglomeration. This suggests that the two-stage dispersion process is effective at this concentration.

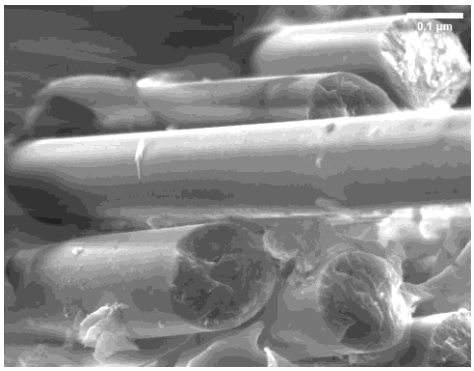

Figure 2. SEM micrographs of the neat epoxy-glass fiber composite at 1500X magnification (EP showing the glass fibers and the smooth, unfilled matrix)

EPC2 (4 wt% $CaCO_3$) & EPC3 (6 wt% $CaCO_3$): As the filler content increased to 4 wt% and 6 wt%, the density of nanoparticles on the fracture surface visibly increased. In these samples, particularly EPC3, the particles still appeared to be reasonably well distributed. They formed a more textured coating on the glass fibers and were embedded throughout the matrix. This increased filler content enhances the tortuosity of the fracture path, which is often associated with improved material toughness. Good dispersion at these loadings is critical for creating a large interfacial area, which facilitates stress transfer and restricts the polymer chain mobility.

EPC4 (8 wt% $CaCO_3$): At the highest loading of 8 wt%, a marked change in morphology is observed. Large agglomerates and clusters of CaCO3 particles became more prevalent. The nanoparticles are no longer well-dispersed individual entities but have formed micron-sized clusters owing to strong inter-particle

van der Waals forces that could not be overcome by the mixing energy at this high concentration. These agglomerates act as stress concentration points and represent defects within the composite structure, which is expected to negatively impact the performance.

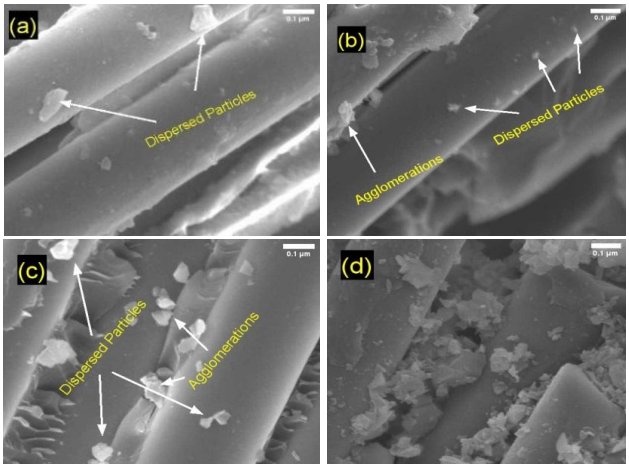

Figure 3. EM micrographs of the single-filler nanocomposites at 1500X magnification: (a) EPC1 (2 wt% $CaCO_3$), (b) EPC2 (4 wt% $CaCO_3$), (c) EPC3 (6 wt% $CaCO_3$), and (d) EPC4 (8 wt% $CaCO_3$). Note the increasing particle density and the onset of agglomeration in (d).

3.1.3. Hybrid-Filler Nanocomposites (EPCT Series) The EPCT series (Fig. 4) introduces nano-talc alongside nano-$CaCO_3$, creating a more complex morphology.

EPCT1 (2% $CaCO_3$ + 1% Talc) & EPCT2 (4% $CaCO_3$ + 2% Talc): At lower hybrid concentrations, the dispersion is excellent. The nanoparticles appeared to create a robust interface between the glass fibers and epoxy matrix. The presence of two different filler types did not seem to impede dispersion; in fact, the combination may sterically hinder the agglomeration of each individual filler type. The fracture surface was rougher and more complex than that of neat epoxy, indicating a more energy-intensive fracture process.

EPCT3 (6% $CaCO_3$ + 3% Talc): This formulation shows a dense and uniform distribution of hybrid nanoparticles. The fillers effectively coat the fibers and are well integrated into the matrix. The rough fracture surface suggests strong interfacial adhesion, where the fracture path is forced to navigate around well-bonded fillers.

EPCT4 (8% $CaCO_3$ + 4% Talc): Similar to the EPC4 sample, the highest hybrid filler loading results in significant agglomeration. Large clusters of undifferentiated $CaCO_3$ and talc particles are visible. The benefits of a large interfacial area are lost as the effective particle size increases owing to this clustering. The presence of these large aggregates creates voids and weak points in the composite.

3.2. Thermal Analysis (DSC)

The glass transition temperature (Tg) is a critical parameter for polymer composites because it defines the upper limit of their service temperature. It represents the temperature at which the polymer transitions from a rigid glassy state to a more flexible rubbery state. This transition is directly related to the mobility of the polymer chains.

The DSC thermograms for all nine formulations were analyzed, and the results are summarized in Table 3 and plotted as an overlaid graph in Figure 5.

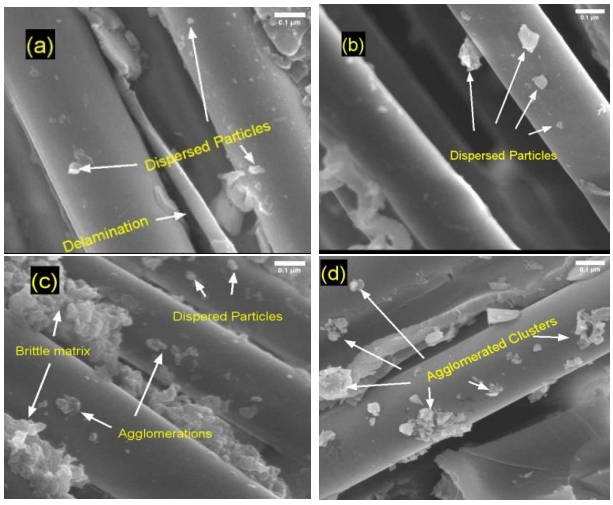

Figure 4. SEM micrographs of the hybrid-filler nanocomposites at 1500X magnification: (a) EPCT1, (b) EPCT2, (c) EPCT3, and (d) EPCT4. Note the good dispersion at lower loadings and significant agglomeration in (d).

Table 3. Glass Transition Temperature (Tg) of the Nanocomposites from DSC Analysis.

Formulation Code	Glass Transition Temp. Tg (°C)
EP	38.17
EPC1	70.15
EPC2	71.66
EPC3	71.70
EPC4	69.74
EPCT1	71.24
EPCT2	72.27
EPCT3	71.81
EPCT4	70.12

As shown in Fig. 5, the neat epoxy composite (EP) exhibits a Tg of 38.17°C marked by a red colored thermogram. A dramatic increase in Tg was observed for all nanocomposite formulations, with values consistently increasing to over 70°C. This substantial increase signifies that the presence of nanofillers, even at low concentrations, significantly restricts the mobility of epoxy polymer chains [27].

3.2.1 Correlation with Morphology: The mechanism behind this increase is the large surface area of the well-dispersed nanoparticles, which creates an extensive interfacial region with the polymer matrix. Within this region, the polymer chains are physically constrained and exhibit reduced mobility compared to the bulk matrix.

In the EPC series, Tg increased from EPC1 to EPC3, peaking at 71.70°C. This trend is consistent with SEM observations. As the filler content increased from 2 wt% to 6 wt%, the volume of the constrained interfacial region increased, leading to a greater restriction of chain motion and thus a higher Tg.

The slight drop in Tg for EPC4 (69.74°C) can be directly attributed to the agglomeration seen in the SEM images. When the nanoparticles agglomerate, the total effective surface area available for interaction with the polymer matrix decreases. The interior

particles within a cluster do not constrain the polymer chains. Therefore, the overall effect of restricting chain mobility is reduced, resulting in a lower Tg compared to that of the well-dispersed EPC3 sample.

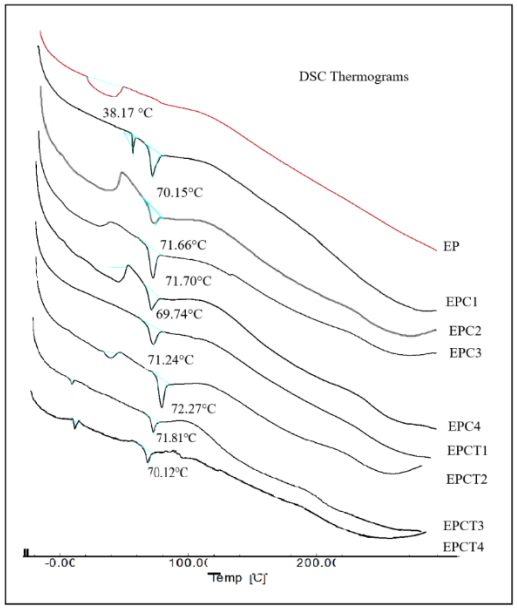

Figure 5. Overlaid DSC curves for all nanocomposite formulations, showing the shift in the glass transition temperature (Tg) with the addition of nanofillers.

The EPCT hybrid series exhibits a similar trend. The Tg is highest for EPCT2 (72.27°C) and EPCT3 (71.81°C), which corresponds to the formulations with good dispersion. The introduction of plate-like talc particles alongside the more equiaxed $CaCO_3$ particles creates a complex network that is highly effective in hindering polymer chain movement. The subsequent drop in EPCT4 (70.12°C) is again explained by the severe agglomeration observed at the highest filler loading.

These results strongly indicate that the nanofillers enhance the thermal stability of the epoxy composites, with the performance being dictated not only by the filler concentration, but also by the quality of dispersion.

3.3. Electrical Properties

The electrical insulation capability of composites is a key performance metric, particularly for applications in electronic and electrical systems. This was evaluated by measuring the dielectric breakdown voltage and surface resistivity.

3.3.1. Dielectric Breakdown Voltage (BDV) dielectric strength measures a material's ability to withstand a high electric field without electrical breakdown. The BDV results for all the formulations are presented in Fig. 6.

The neat epoxy composite (EP) exhibited a BDV of 14.1 kV. The addition of nanofillers has a complex, nonlinear effect on this property.

EPC Series: The BDV increases from 14.3 kV for EPC1 to a peak of 16.6 kV for EPC3, an improvement of nearly 18% over the neat composite. This enhancement can be attributed to the well-dispersed and electrically insulating $CaCO_3$ nanoparticles. These particles act as scattering centers for the charge carriers and create tortuous paths that hinder the formation of a conductive breakdown channel through the material. The strong interface between the fillers and matrix, as suggested by the morphology, also helps to reduce the defects that could initiate breakdown [28-30]. The subsequent drop in the BDV for EPC4 (14.6 kV) correlates directly with the observed agglomeration. Agglomerates introduce defects and create weak points at the interface between the cluster and matrix, which can act as initiation sites for electrical breakdown at lower voltages. As concentration of nanoparticles increases, the inter-particle distance decreases, leading to cluster formation. These agglomerates act as defects that distort the local electric field (field enhancement), creating localized stress points where breakdown can initiate. Additionally, voids or weak boundaries associated with these agglomerates serve as easier pathways for electrical treeing, outweighing the barrier benefits of the fillers [31,32].

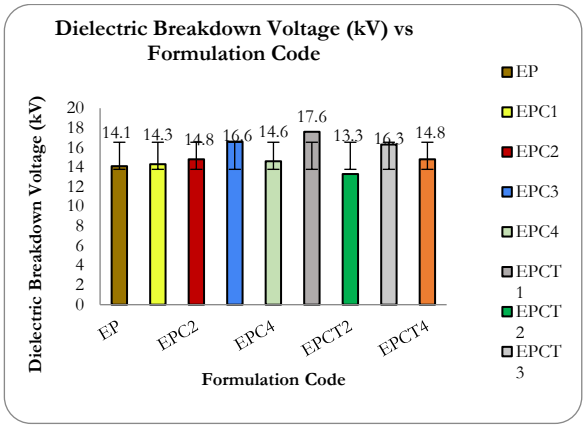

Figure 6. Dielectric Breakdown Voltage (kV) for all nanocomposite formulations. Error bars represent standard deviation.

EPCT Series: The hybrid fillers exhibited a remarkable effect at low concentrations. EPCT1 (2% $CaCO_3$ + 1% Talc) exhibits the highest BDV of all samples at 17.6 kV, a 25% improvement over the neat composite. This suggested a powerful synergistic effect. This is partly due to the plate-like Talc creating a barrier structure and the spherical CaCO3 improving toughness. The combination disrupts electrical breakdown pathways more effectively than single-shape fillers. However, as the concentration increased, the BDV decreased significantly, with EPCT2 exhibiting the lowest value (13.3 kV) before recovering slightly for EPCT3 and EPCT4. This sharp drop, despite the good dispersion seen in EPCT2's morphology, may be due to the introduction of more interfaces, which can sometimes trap charge or moisture or the specific dielectric properties of talc. The overall trend highlights the sensitivity of the dielectric properties to both filler type and concentration [33,34].

3.3.2. Surface Resistivity

Surface resistivity measures the resistance to the leakage current flowing along the surface of an insulator. A high surface resistivity is desirable for insulation applications. The results are plotted on a logarithmic scale in Fig. 7 owing to the large variation in magnitude.

The neat epoxy composite (EP) exhibited a very high surface resistivity of 36.59×1012 Ω. Interestingly, the addition of nanofillers generally leads to a decrease in the surface resistivity, with values dropping by several orders of magnitude for most

formulations. This reduction is likely due to the introduction of a large number of filler-polymer interfaces. While the fillers themselves are insulators, the interfacial regions can facilitate charge transport or attract polar molecules, such as water, from the atmosphere. This adsorbed moisture can create a slightly conductive pathway on the surface, thereby lowering the overall resistivity.

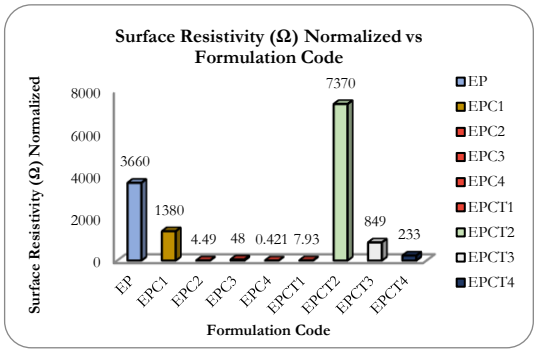

Figure 7. Surface Resistivity (Omega) for all nanocomposite formulations, plotted on a logarithmic scale.

The EPC series showed a significant drop in resistivity, particularly for EPC2 and EPC4, which fell to the 109−108 Ω range. This may relate to the specific surface chemistry of the stearic acid-treated CaCO3 [35,36].

The EPCT series showed a more complex behavior. While EPCT1 shows a low resistivity, EPCT2 recovers significantly to 73.74×1012 Ω, a value even higher than that of the neat epoxy. This is an exceptional result, suggesting that the specific combination of 4 wt% $CaCO_3$ and 2 wt% talc, which was well dispersed, creates a surface that is highly resistant to charge leakage. The plate-like nature of talc may play a role in disrupt the formation of continuous conductive surface paths. As the concentration increased further in EPCT3 and EPCT4, the resistivity decreased again, likely owing to the onset of agglomeration and an increase in interfacial defects.

The electrical property results underscore the complexity of the nanocomposite behavior. Although fillers enhance the bulk dielectric strength (BDV) by acting as barriers, they can decrease the surface resistivity by introducing numerous interfaces. The optimal formulation depends on the specific electrical properties targeted.

3.4. Flammability Analysis

The flammability of the composites was evaluated using the UL 94 vertical burn test. The results were straightforward: all nine formulations, including the neat epoxy control, achieved a V-1 rating.

A V-1 rating indicates that for a vertically mounted specimen, burning stops within 30 s after the flame source is removed and flaming drips are not allowed. While the inclusion of mineral nanofillers did not improve the rating to the more stringent V-0 category, it is crucial to note that they did not degrade the performance. The mechanism by which mineral fillers act as flame retardants has been well established. During combustion, they can be Act as a Heat Sink: The Inorganic particles absorb thermal energy, slowing the temperature rise of the polymer and delaying its thermal decomposition into flammable volatile gases.

Release Inert Gases: Hydrated minerals like talc ($Mg_3Si_4O_{10}(OH)_2$) can release water vapor at high temperatures. Carbonates like $CaCO_3$ release carbon dioxide. These inert gases dilute the flammable gases and oxygen in the combustion zone, thereby suppressing the flame.

Form a Protective Char Layer: The accumulated mineral fillers on the surface can form a physical barrier (char layer) that insulates the underlying polymer from the heat source and slows the escape of flammable volatiles.

While these effects were not potent enough to achieve a V-0 rating in this study, they likely contributed to the maintenance of the V-1 classification. It is possible that at concentrations higher than those tested, or with different mineral filler types (such as aluminum hydroxide), a more significant improvement in flame retardancy could be achieved. The consistent V-1 rating across all the samples indicates that the composites possess a reliable and stable level of fire resistance suitable for many applications.

3.5. Comparison with Existing Studies

To provide context for the performance of the synthesized nanocomposites, the findings were compared with recent studies on both single-filler and hybrid systems documented in the literature. In terms of electrical insulation, the optimal hybrid formulation (EPCT1) demonstrated a notable enhancement in Dielectric Breakdown Voltage (BDV), achieving 17.6 kV. This synergistic improvement is consistent with recent reviews on hybrid filler systems, which suggest that the integration of fillers with varying aspect ratios (such as platelets and spheres) establishes a more efficient "tortuous path" for charge carriers compared to single-filler systems, thus delaying breakdown [25].

Regarding thermal properties, the substantial rise in Glass Transition Temperature (Tg) noted in our hybrid system (up to 72.27°C) sets it apart from numerous single-filler investigations. For example, recent studies on nano-$CaCO_3$/epoxy composites indicated that while the addition of single fillers enhanced flexural strength, the improvements in thermal stability were frequently constrained by particle agglomeration at elevated loadings [22]. Moreover, a 2025 study on ternary/hybrid epoxy nanocomposites revealed that synergistic interactions among fillers are essential for achieving optimal thermal stability, as they more effectively limit polymer chain mobility compared to individual fillers [26]. Our results corroborate this observation, indicating that the combination of nano-talc and nano-$CaCO_3$ mitigates the deficiencies associated with single-filler systems.

3.6. Economic Evaluation and Application Benefits

The development of hybrid nanocomposites is driven not only by performance enhancement but also by cost-effectiveness. Epoxy resin is a relatively expensive engineering polymer compared to mineral fillers. The incorporation of naturally abundant mineral fillers, such as CaCO3 and Talc, offers a distinct economic advantage. By substituting a portion of the expensive epoxy matrix with low-cost nanofillers (up to 8 wt% in this study), the overall material cost of the component can be reduced without compromising—and in many cases, enhancing—critical properties. Unlike expensive nanofillers like Carbon Nanotubes (CNTs) or Graphene, mineral fillers provide a scalable solution for industrial mass production.

In terms of applications, the specific property profile observed in this study opens several avenues. The hybrid formulation (EPCT1), which exhibited a dielectric breakdown voltage of 17.6 kV10, is highly suitable for high-voltage electrical insulation, such as switchgear components, insulators, and circuit breaker housings. Furthermore, the enhanced thermal stability (Tg > 70°C) and V-1 flame retardancy make these composites ideal candidates for electronic packaging materials and printed circuit board (PCB) substrates, where resistance to heat generation and electrical failure is paramount.

4. Conclusion

In this study, a series of epoxy-glass fiber nanocomposites were reinforced with single (nano-$CaCO_3$) and hybrid (nano-$CaCO_3$ + nano-talc) filler systems. This research provides a focused analysis of the morphological, thermal, and electrical properties, leading to the following key conclusions:

Morphology is Key: The dispersion of nanofillers is a critical factor governing the composite performance. SEM analysis confirmed that good dispersion was achievable at low to moderate filler loadings (up to 6 wt% total), while higher concentrations (>8 wt%) led to significant agglomeration, which created defects and compromised the properties.

Enhanced Thermal Stability: The incorporation of nanofillers resulted in a substantial increase in the glass transition temperature (Tg) by over 30°C compared with that of the neat epoxy composite. This enhancement, attributed to the physical restriction of polymer chain mobility at the large filler-matrix interfacial area, confirms the improved thermal stability of the nanocomposites. The Tg peak was observed in well-dispersed systems, with a subsequent decrease when agglomeration occurred.

Tailorable Electrical Properties: The Nanofillers have a profound and tunable impact on the electrical insulation properties. Dielectric Strength was significantly improved, with the hybrid formulation EPCT1 (2% $CaCO_3$ + 1% Talc) showing a 25% increase in breakdown voltage over the neat composite. This demonstrates that a synergistic combination of fillers is highly effective at disrupting the electrical breakdown pathways, even at low concentrations. Surface Resistivity, however, generally decreases with filler addition owing to the creation of interfacial pathways. A notable exception was the EPCT2 formulation (4% $CaCO_3$ + 2% Talc), which exhibited the highest surface resistivity, suggesting an optimal hybrid combination for minimizing surface current leakage.

Consistent Flammability: All fabricated composites, regardless of filler content, maintained a UL 94 V-1 flammability rating, indicating a reliable level of fire resistance that was not degraded by filler addition.

In summary, this work demonstrates that the use of hybrid nano-$CaCO_3$ and nano-talc fillers is a highly effective strategy for engineering the properties of epoxy-glass fiber composites. The performance is not merely a function of filler concentration, but is a complex interplay between filler type, concentration, and, most importantly, the resulting dispersion morphology. The findings highlight that an optimal balance can be achieved, for example, in the formulation of EPCT1 for dielectric strength and EPCT2 for surface resistivity, showcasing the potential to develop cost-effective, high-performance materials tailored for specific applications in the electrical, electronic, and automotive industries.

5. References

[1] S. Das, "The Cost of Automotive Polymer Composites: A Review and Assessment of DOE's Lightweight Materials Composites Research," Office Of Scientific Technical Information, Jan. 2001. https://doi.org/10.2172/777656

[2] K. Agarwal, M. Houser, S. K. Kuchipudi, and B. Girard, "Mechanical properties of fiber reinforced polymer composites: A comparative study of conventional and additive manufacturing methods," Journal of Composite Materials, vol. 52, no. 23, pp. 3173–3181, Mar. 2018, https://doi.org/10.1177/0021998318762297

[3] C. Wu, F. Xu, H. Wang, H. Liu, F. Yan, and C. Ma, "Manufacturing Technologies of Polymer Composites—A Review," Polymers, vol. 15, no. 3, p. 712, Jan. 2023, https://doi.org/10.3390/polym15030712

[4] J. G. Gwon, G. H. Doh, S. J. Chun, S. Y. Lee, and J. H. Kim, "Physical and mechanical properties of wood–plastic composites hybridized with inorganic fillers," Journal of Composite Materials, vol. 46, no. 3, pp. 301–309, Sept. 2011, https://doi.org/10.1177/0021998311413690

[5] R. Olayil, O. Das, V. Arumugaprabu, and W. A. Lenin Anselm, "A Brief Review on Effect of Nano fillers on Performance of Composites," IOP Conf. Ser.: Mater. Sci. Eng., vol. 1059, no. 1, p. 012006, Feb. 2021, https://doi.org/10.1088/1757-899x/1059/1/012006

[6] M. Z. Rong, M. Q. Zhang, and W. H. Ruan, "Surface modification of nanoscale fillers for improving properties of polymer nanocomposites: a review," Materials Science and Technology, vol. 22, no. 7, pp. 787–796, July 2006, https://doi.org/10.1179/174328406x101247

[7] Y. Wang, R. J. Macfarlane, and G. J. Desroches, "Ordered polymer composite materials: challenges and opportunities.," Nanoscale, vol. 13, no. 2, pp. 426–443, Jan. 2021, https://doi.org/10.1039/d0nr07547g

[8] A. Haque, D. Dean, M. Shamsuzzoha, and F. Hussain, "S2-Glass/Epoxy Polymer Nanocomposites: Manufacturing, Structures, Thermal and Mechanical Properties," Journal of Composite Materials, vol. 37, no. 20, pp. 1821–1837, Oct. 2003, https://doi.org/10.1177/002199803035186

[9] Y. Liu and S. Li, "Using silica nanoparticles as curing reagents for epoxy resins to form epoxy–silica nanocomposites," J of Applied Polymer Sci, vol. 95, no. 5, pp. 1237–1245, Jan. 2005, https://doi.org/10.1002/app.21327

[10] S. Mishra, S. Sonawane, and V. Chitodkar, "Comparative Study on Improvement in Mechanical and Flame Retarding Properties of Epoxy-CaCO3 Nano and Commercial Composites," Polymer-Plastics Technology and Engineering, vol. 44, no. 3, pp. 463–473, Mar. 2005, https://doi.org/10.1081/pte-200048299

[11] N. Sharma, V. Singal, and D. D'Melo, "Evaluation of water vapour permeability of solventless epoxy – nano talc/montmorrilonite amino-silane coupled coatings,"

Pigment & Resin Technology, vol. 42, no. 1, pp. 45–52, Jan. 2013, https://doi.org/10.1108/03699421311288751

[12] M. Kolahdouz et al., "Carbon-Related Materials: Graphene and Carbon Nanotubes in Semiconductor Applications and Design," Micromachines, vol. 13, no. 8, p. 1257, Aug. 2022, https://doi.org/10.3390/mi13081257

[13] J. R. and J. W. Gillespie Jr., "Fracture Behaviors of Graphene Sheets and Carbon Nanotubes," Institute for New Technologies, 2011. https://doi.org/10.5772/14948

[14] I. Tsekmes, "Analysis of the Mechanisms Determining the Thermal and Electrical Properties of Epoxy Nanocomposites for High Voltage Applications," Jan. 2016, https://doi.org/10.4233/uuid:c07dbb22-09c1-432b-a48a-4b122568143e

[15] S. Thipperudrappa, A. Ullal Kini, and A. Hiremath, "Influence of zinc oxide nanoparticles on the mechanical and thermal responses of glass fiber-reinforced epoxy nanocomposites," Polymer Composites, vol. 41, no. 1, pp. 174–181, Aug. 2019, https://doi.org/10.1002/pc.25357

[16] S. Sugiman, S. Salman, A. Dwi Catur, and Y. Panca Asmara, "Modelling the flexural properties of filled epoxy: Effects of volume fraction," E3S Web of Conf., vol. 465, p. 01028, Jan. 2023, https://doi.org/10.1051/e3sconf/202346501028

[17] F. N. Ahmad, M. Jaafar, S. Palaniandy, and K. A. M. Azizli, "Effect of particle shape of silica mineral on the properties of epoxy composites," Composites Science and Technology, vol. 68, no. 2, pp. 346–353, Aug. 2007, https://doi.org/10.1016/j.compscitech.2007.07.015

[18] A. S. Prasad et al., "Investigating the effect of surface modification on the dispersion process of polymer nanocomposites," Nanocomposites, vol. 6, no. 3, pp. 111–124, Aug. 2020, https://doi.org/10.1080/20550324.2020.1809250

[19] M. De Oliveira Taipina, I. V. P. Yoshida, M. D. C. Gonçalves, and M. M. F. Ferrarezi, "Surface modification of cotton nanocrystals with a silane agent," Cellulose, vol. 20, no. 1, pp. 217–226, Feb. 2013, https://doi.org/10.1007/s10570-012-9820-3

[20] Y. Pan, M. Zhang, H. Bian, C. Wang, X. Zhu, and J. Zhang, "Effect of Silane Coupling Agent on Modification of Areca Fiber/Natural Latex.," Materials, vol. 13, no. 21, p. 4896, Oct. 2020, https://doi.org/10.3390/ma13214896

[21] A. Fihri et al., "Effect of interfacial modification on functional properties of polyethylene and polypropylene—Fibrous silica nanocomposites," Vinyl Additive Technology, vol. 30, no. 3, pp. 653–662, Dec. 2023, https://doi.org/10.1002/vnl.22076

[22] A. Misra, M. Shukla, M. K. Shukla, D. Srivastava, and A. K. Nagpal, "Nano CaCO3 modified multifunctional epoxy nanocomposites: A study on flexural and structural properties," Materials Today: Proceedings, vol. 47, pp. 3295–3300, Jan. 2021, https://doi.org/10.1016/j.matpr.2021.07.143

[23] N. Hammad, A. El-Nemr, and I. G. Shaaban, "The Efficiency of Calcium Oxide on Microbial Self-Healing Activity in Alkali-Activated Slag (AAS)," Applied Sciences, vol. 14, no. 12, p. 5299, June 2024, https://doi.org/10.3390/app14125299

[24] Y. W. Leong, A. Ariffin, and Z. A. M. Ishak, "Mechanical and thermal properties of talc and calcium carbonate filled polypropylene hybrid composites," J of Applied Polymer Sci, vol. 91, no. 5, pp. 3327–3336, Jan. 2004, https://doi.org/10.1002/app.13543

[25] O. A. Afolabi and N. Ndou, "Synergy of Hybrid Fillers for Emerging Composite and Nanocomposite Materials-A Review.," Polymers, vol. 16, no. 13, p. 1907, July 2024, https://doi.org/10.3390/polym16131907

[26] A. A. Patil, P. S. Shisode, A. S. Patil, A. A. Patil, P. P. Mahulikar, and C. B. Patil, "Impact of bio-filler concentration on the thermal and mechanical properties of epoxy nanocomposites," Bull Mater Sci, vol. 48, no. 2, Apr. 2025, https://doi.org/10.1007/s12034-025-03421-6

[27] W. Silva Dias et al., "3D Printing of Virucidal Polymer Nanocomposites (PLA/Copper Nanoparticles).," Polymers, vol. 17, no. 3, p. 283, Jan. 2025, https://doi.org/10.3390/polym17030283

[28] I. Pleşa, P. V. Noţingher, S. Schlögl, C. Sumereder, and M. Muhr, "Properties of Polymer Composites Used in High-Voltage Applications," Polymers, vol. 8, no. 5, p. 173, Apr. 2016, https://doi.org/10.3390/polym8050173

[29] S. Nait Larbi et al., "Characterization of PVC/CaCO3 Nanocomposites Aged Under the Combined Effects of Temperature and UV-Radiation," Materials, vol. 18, no. 17, Aug. 2025, https://doi.org/10.3390/ma18174001

[30] J. Yao et al., "Synchronously Strengthen and Toughen Polypropylene Using Tartaric Acid-Modified Nano-CaCO3.," Nanomaterials, vol. 11, no. 10, p. 2493, Sept. 2021, https://doi.org/10.3390/nano11102493

[31] M. Danikas, "Breakdown in Nanofluids: A Short Review on Experimental Results and Related Mechanisms," Eng. Technol. Appl. Sci. Res., vol. 8, no. 5, pp. 3300–3309, Oct. 2018, https://doi.org/10.48084/etasr.2136

[32] S. Sorte, A. Salgado, A. F. Monteiro, D. Ventura, N. Martins, and M. S. A. Oliveira, "Advancing Power Transformer Cooling: The Role of Fluids and Nanofluids—A Comprehensive Review," Materials, vol. 18, no. 5, p. 923, Feb. 2025, https://doi.org/10.3390/ma18050923

[33] R. Wang, C. Xie, S. Luo, B. Gou, H. Xu, and L. Zeng, "The influence mechanism of nanoparticles on the dielectric properties of epoxy resin.," RSC Adv., vol. 9, no. 34, pp. 19648–19656, Jan. 2019, https://doi.org/10.1039/c9ra02889g

[34] A. Fajdek-Bieda and A. Wróblewska, "The Use of Natural Minerals as Reinforcements in Mineral-Reinforced Polymers: A Review of Current Developments and Prospects," Polymers, vol. 16, no. 17, p. 2505, Sept. 2024, https://doi.org/10.3390/polym16172505

[35] C.-Q. Li et al., "Surface modification of calcium carbonate: A review of theories, methods and applications," J. Cent. South Univ., vol. 28, no. 9, pp. 2589–2611, Sept. 2021, https://doi.org/10.1007/s11771-021-4795-6

[36] U. Sundar, Z. Lao, and K. Cook-Chennault, "Investigation of Piezoelectricity and Resistivity of Surface Modified Barium Titanate Nanocomposites," Polymers, vol. 11, no. 12, p. 2123, Dec. 2019, https://doi.org/10.3390/polym11122123